J. Serb. Chem. Soc. 69 (10) 807–815 (2004)
JSCS – 3207

UDC 546.72–034.5:621.357:620.123
Original scientific paper

Electrochemical deposition and characterization of Zn–Fe alloys

JELENA B. BAJAT[1,#], VESNA B. MIŠKOVIĆ-STANKOVIĆ[1,*#], MIODRAG D. MAKSIMOVIĆ[1], DAGUTIN M. DRAŽIĆ[2,#] and SLAVICA ZEC[3]

[1]Faculty of Technology and Metallurgy, University of Belgrade, Karnegijeva 4, P.O. Box 3503, 11120 Belgrade, [2]ICTM – IEC, P.O.Box 815, 11001 Belgrade and [3]Vinča Institute of Nuclear Sciences, P.O. Box 522, 11001 Belgrade, Serbia and Montenegro (e-mail: vesna@tmf.bg.ac.yu)

(Received 7 May 2004)

Abstract: Zn–Fe alloy electrochemically deposited on steel under various deposition conditions were investigated using anodic linear sweep voltammetry (ALSV) and X-ray diffraction (XRD) analysis for phase structure determination, energy dispersive X-ray (EDX) analysis for determination of chemical composition, and polarization measurements and open circuit potential measurements for determination of corrosion properties. The influence of deposition current density on the chemical composition, phase structure and corrosion stability of Zn–Fe alloys was studied. It was shown that deposition current density strongly affects the corrosion stability of Zn–Fe alloys, while Zn–Fe alloy electrodeposited at 4 A dm^{-2} exhibited the lowest corrosion rate.

Keywords: electrodeposition, Zn–Fe alloy, corrosion, surface modification.

INTRODUCTION

Among variety of coating types, zinc coating is widely used as a protective coating on steel and one of the very important problems in galvanizing is the improvement of the protective and functional properties of Zn coatings. According to literature[1–3] zinc alloys can provide improved corrosion resistance compared to pure zinc in the protection of ferrous-based metals. This is easily achieved by alloying Zn with more noble metals, mostly with metals of the iron group (Ni, Co and Fe).[4,5] Among them, zinc–iron alloys have been used a lot recently, since they showed excellent corrosion resistance (due to the nature of the zinc–iron phase), good paintability, formability and weldability (due to the high hardness and melting point of the zinc–iron phase in comparison to pure zinc) and ease of formation of the coating.[6,7] Zinc–iron alloys exist in various phases and their structure and morphology[8] also determine the corrosion resistance of a deposit.

The aim of this work was to modify a steel surface by electrodeposition of the Zn–Fe

Corresponding author.

* Serbian Chemical Society active member.

alloy exhibiting the best corrosion protective properties, prior to epoxy coating deposition. Emphasis was placed on determining the electroplating conditions whereby the Zn–Fe alloy with the best corrosion resistance would be obtained. This alloy was then used as a sublayer for epoxy coating electrodeposition.

EXPERIMENTAL

Electrodeposition of Zn–Fe alloys

Zn–Fe alloys were deposited galvanostatically at 0.5 – 15.0 A dm^{-2}, on a steel panel or on a rotating disc electrode at 25 and 40 ºC from alkaline bath: 0.09 mol dm^{-3} $ZnSO_4$, 0.01 mol dm^{-3} $FeSO_4$, 0.01 mol dm^{-3} ascorbic acid, ≈0.2 mol dm^{-3} triethanolamine, 30 g dm^{-3} Na_2SO_4 and 80 g dm^{-3} NaOH (pH ≈ 14).[8] The employed electrolyte was prepared using p.a. chemicals (Merck, Aldrich, Fluka) and double distilled water.

The working electrodes were as follows:

a) A steel and steel modified by Zn–Fe alloy panels (20 mm × 20 mm × 0.25 mm), for measurements of the open circuit potential. The steel panel surface was pretreated by mechanical cleaning (polishing successively with emery papers of the following grades: 280, 360, 800 and 1000) and then degreased in a saturated solution of sodium hydroxide in ethanol, pickled with a 1 : 1 hydrochloric acid solution for 30 s and finally rinsed with distilled water.

b) A steel and steel modified by Zn–Fe alloy rotating disc electrodes (d = 8 mm, at 2000 rpm), for polarization measurements. The steel disc surface was pretreated in the same manner as the steel panel surface, described above.

c) A Pt rotating disc electrode (d = 8 mm, at 2000 rpm), for anodic linear sweep voltammetry (ALSV). Prior to each electrodeposition, the Pt disc surface was mechanically polished with a polishing cloth (Buehler Ltd.), impregnated with a water suspension of alumina powder (0.3 μm grade) and then rinsed with pure water in an ultrasonic bath.

d) A Cu rotating disc electrode (d = 6 mm, at 2000 rpm), for X-ray diffraction measurements. Prior to each electrodeposition, the Cu disc surface was pretreated in the same manner as the Pt disc surface, described above.

Counter electrodes were as follows:

a) Zinc panels (high purity zinc, 30 mm × 30 mm × 0.15 mm), placed parallel to the steel panel electrode at a distance of 1.5 cm (for plating on a panel).

b) A zinc spiral ribbon (high purity zinc, surface area 8 cm^2), placed parallel to the RDEs at a distance of 1.5 cm (for plating on a rotating disc electrode).

c) A Pt spiral wire for polarization and corrosion measurements.

The reference electrode used in all experiments was a saturated calomel electrode (SCE). All the potentials are referred against SCE. The thickness of Zn–Fe alloys was 10 μm.

The chemical composition of the Zn–Fe alloys was determined by EDX analysis of the deposits, using Scanning Electron Microscopy (SEM) type PHILIPS XL 30.

Anodic linear sweep voltammetry (ALSV)

For alloy phase structure determination alloys were dissolved anodically at room temperature (23 ± 1 ºC) using a slow sweep voltammetry technique (sweep rate 1 mV s^{-1} and rotation of 2000 rpm)[9] in N_2 saturated 0.5 mol dm^{-3} Na_2SO_4 + 0.05 mol dm^{-3} EDTA solution.

Phase structure determination

The phases present in the deposits and the preferred orientation of the deposits were determined by X-ray diffraction (XRD) analysis, using a Siemens D500 X-ray diffractometer with CuK_αNi-filtered radiation. The 2θ range of 20–100º was recorded at the rate of 0.02º 2θ/0.5 s. The crystal phases were identified comparing the 2θ values and intensities of reflections on X-ray diffractograms with JCP data base using a Diffrac AT-Siemens program.

Corrosion measurements

The corrosion rates in a dearated 3 % NaCl solution (N_2 was bubbled for 15 min prior to all experiments) of the electrodeposited Zn–Fe alloys were determined using extrapolation of anodic polarization curves to the open circuit potential. Potential sweep rate of 2 mV s^{-1} (rotation of 2000 rpm) was applied starting from the open circuit potential, E_{ocp}, after the constant E_{ocp} was established (up to 20 min).

Determination of the rate of H_2 evolution reaction

The rate of hydrogen evolution reaction in the polymer solution on steel and Zn–Fe surfaces was determined using a slow sweep voltammetry (sweep rate 0.5 mV s^{-1}, rotation of 2000 rpm). The working electrode used in this experiment was a either steel or Pt rotating disc electrode (d = 8 mm). The steel disc surface was prepared in the same manner as the steel panels.

RESULTS AND DISCUSSION

Alloy characterization

Preliminary experiments were related to deposition of Zn–Fe alloys at different deposition current density and temperature of plating bath and, based on the appearance of deposits certain deposition parameters were chosen for further alloy investigation. When deposition was carried out at 2.0–10.0 A dm^{-2}, homogeneous and coherent coatings were obtained at 25 ºC. Above this temperature (at 30, 35 and 40 ºC) and above 10 A dm^{-2} (at all temperatures) deposits appeared less uniform, with rough, spongy (powdery) deposits around the edges of the samples. Homogeneous, gray deposits were obtained at 2.0–10.0 A dm^{-2}. Deposits obtained at lower current densities, 0.5 and 1.0 A dm^{-2} had visible vertical white lines spread along the working panel, probably due to the hydrogen evolution, as a parallel cathodic reaction during electrochemical plating. These lines were not present for $j \geq 2$ A dm^{-2}, when H_2 bubble formation is more uniform over the surface.

Anodic linear sweep voltammetry (ALSV) was used in determining the phase structure of Zn–Fe alloys.[9,10] When an alloy film is polarized anodically under potentiodynamic conditions, the components dissolve at various potentials, depending on their equilibrium and kinetic properties. The various phase structures and chemical forms present in the alloy produce various current peaks. Therefore, an obtained peak structure is a characteristic of the alloy componenets and the phase structure of the deposit. The ALSVs, obtained in Na_2SO_4 + EDTA solution, for the Zn–Fe alloys deposited at various current densities are shown in Fig. 1a. Voltammetric dissolution peaks of pure Zn and Fe components are also shown in Fig. 1b, along with the ALSV for Zn–Fe alloy deposited at 4 A dm^{-2}. The alloy dissolution takes place mainly under one voltammetric peak, denoted as I in Figs. 1a and 1b, for all investigated Zn–Fe deposits, although there is a shoulder, denoted as I', in Fig. 1a.

The chemical composition of the Zn–Fe alloys was determined by EDX analysis of the deposits using SEM and varied from 1.0 wt.%, for ally electrodeposited at 2 A dm^{-2}, to 2.2 wt.%, for alloy electrodeposited at 10 A dm^{-2}.

On the basis of ALSVs, chemical composition and equilibrium phase diagram,[11] it was shown that all alloys consist of one phase, Zn-rich η-phase. Namely, it is supposed that the current peak I is due to the preferential dissolution of Zn from solid solution of Zn–Fe alloy, while peak I' corresponds to the removal of the porous Fe matrix (*i.e.*, to the dissolu-

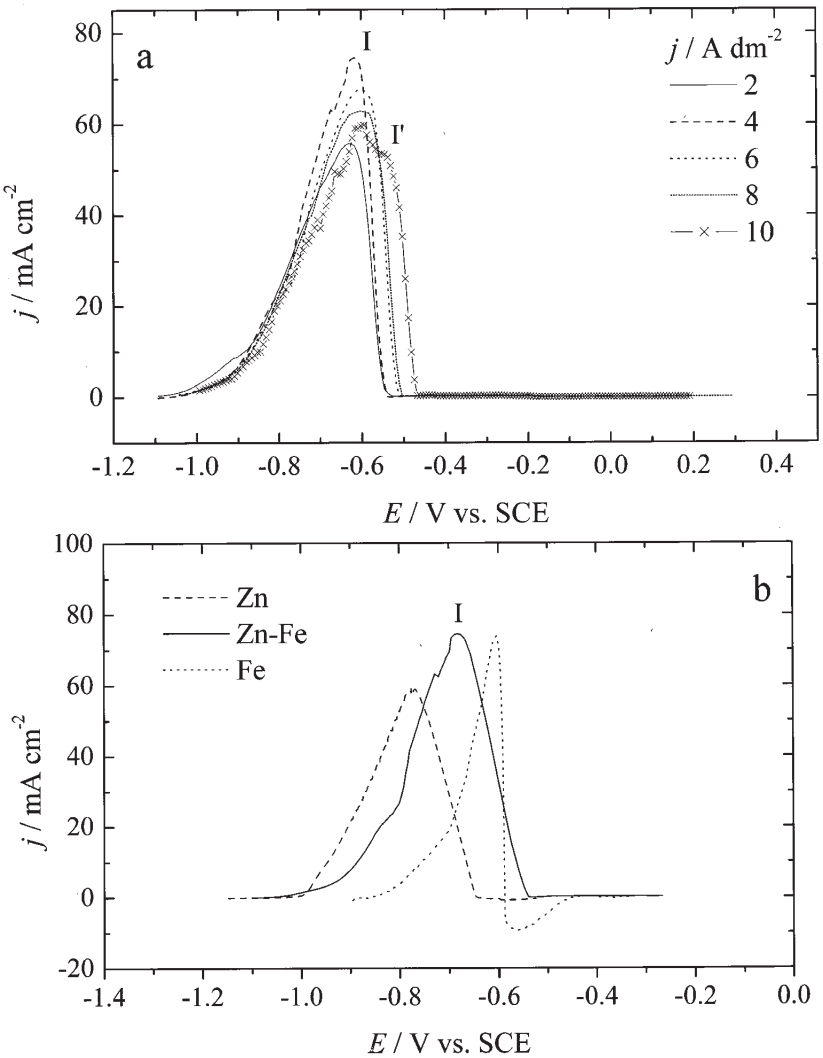

Fig. 1. ALSV voltammograms in Na_2SO_4 + EDTA solution of dissolution of: (a) Zn–Fe alloys deposited at different current densities, and (b) Zn, Fe and Zn–Fe alloy deposited at 4 A dm^{-2} (sweep rate 1 mV s^{-1}, 2000 rpm).

tion of the remaining alloy phase richer in Fe). Shoulder I' appears only in the case of Zn–Fe alloy deposited at 10 A dm^{-2}, since this is the alloy with the greatest Fe content of all investigated (2.2 wt.%).

The Zn–Fe alloy coatings have the same structure as zinc,[1] but with different crystallographic orientation, which is the consequence of the small iron amount. The X-ray diffractograms of Zn–Fe coatings deposited at three different current densities are shown in Fig. 2. The reflections of zinc rich η-phase (JCP: 4-0831)[12] are present in all investigated deposits. The (002) reflection is not present on X-ray diffractograms of deposits ob-

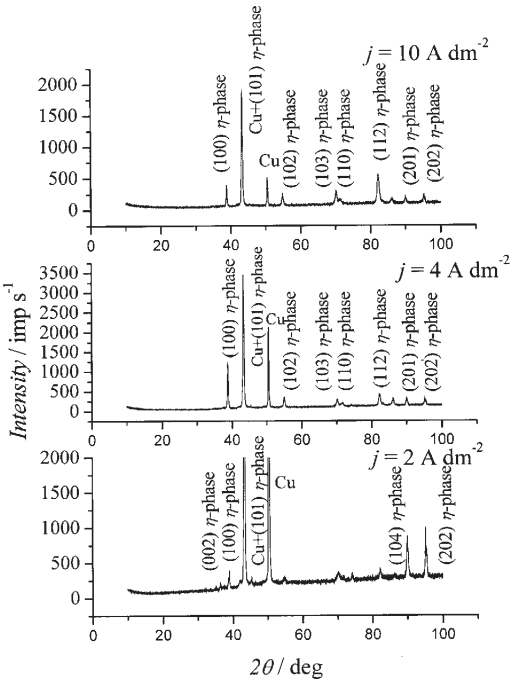

Fig. 2. X-Ray diffraction patterns of the Zn–Fe alloys deposited at different current densities.

tained at 4 and 10 A dm^{-2}, while intensities of (100) and (101) reflections are greater, especially for Zn–Fe alloy deposited at 4 A dm^{-2}.

Corrosion properties of Zn–Fe alloys

The steel panels were modified by electrodeposition of Zn–Fe alloys at different current densities and the plated specimens were immersed in a 3 % aqueous NaCl solution. The open circuit potential, E_{ocp}, was measured daily in order to investigate the corrosion resistance of the Zn–Fe alloys (Fig. 3). The potentials of Zn–Fe alloys are more negative than that of steel (–0.640 V *vs.* SCE) under the same conditions, so Zn–Fe alloys offer saccrificial cathodic protection. Basically, corrosion potentials of all Zn–Fe alloys are very negative compared to steel surface, since there is only a little amount of Fe in an alloy. Still, Zn–Fe alloy offers a good corrosion protection.

The E_{ocp} values of steel modified by Zn–Fe alloys increase positively with time of immersion and reach the E_{ocp} value of bare steel which represents loss of the alloy deposit and the start of a corrosion process on still. The results of the visually observed alloy destruction in 3 % NaCl solution, or the appearance of the red rust on the steel, are presented in Table I. Of all deposits, the one deposited at 10 A dm^{-2} was destroyed first. The alloy deposited at 4 A dm^{-2} lasted the longest, 29 days.

TABLE I. The time of red rust appearance for Zn–Fe alloys deposited at different current densities

j / A dm^{-2}	2	4	6	8	10
Time / days	25	29	17	15	14

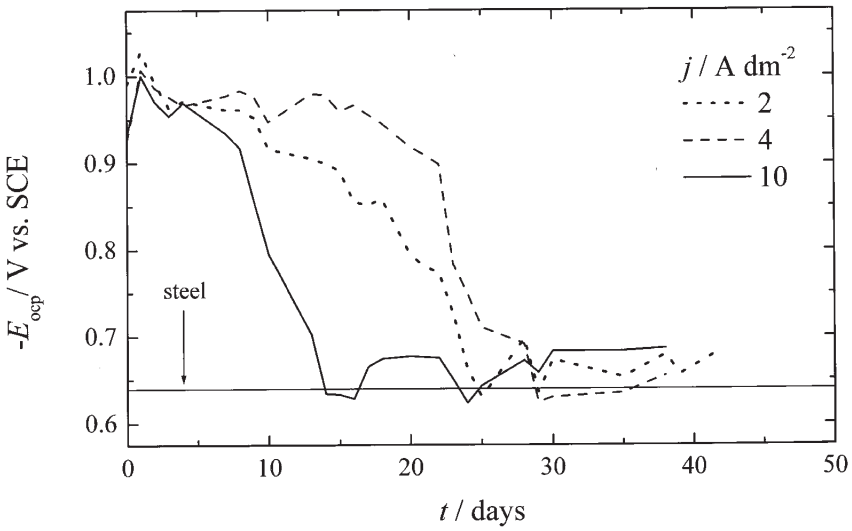

Fig. 3. Time dependence of E_{ocp} in 3 % NaCl for steel modified by Zn–Fe alloys deposited at different current densities.

Anodic polarization curves in a small range of potential near to E_{ocp} were obtained in a 3 % NaCl solution (Fig. 4). The corrosion current densities, j_{corr}, were estimated from the intersections of the anodic Tafel plots with the E_{ocp}. The corrosion potentials, E_{corr} and corresponding corrosion current densities, j_{corr}, for the Zn–Fe alloys deposited at different current densities are given in Table II. Data in Table II are mean values of three to five measurements.

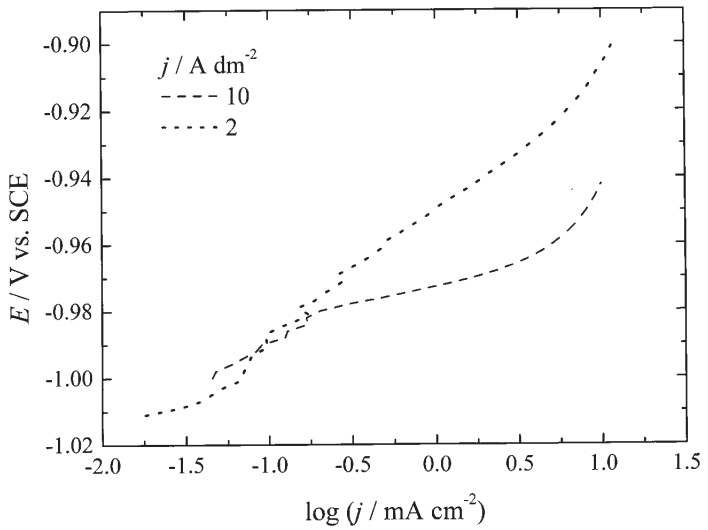

Fig. 4. Anodic polarization curves in 3 % NaCl for Zn–Fe alloys deposited at 2 and 10 A dm^{-2} (sweep rate 2 mV s^{-1}, 2000 rpm).

TABLE II. Corrosion potentials, E_{corr} and corrosion current densities, j_{corr}, of Zn–Fe alloys electrodeposited at different current densities*

j / A dm^{-2}	2	4	6	8	10
$-E_{corr}$ / V *vs.* SCE	1.012	1.040	1.048	1.048	1.000
j_{corr} / μA cm^{-2}	45	30	48	50	50

*Data are mean values of three to five measurements

Chemical composition, obtained by EDX analysis, showed that the Fe amount is the greatest in the case of alloy deposited at 10 A dm^{-2} (2.2 wt.%, whereas it was 1.3 wt.% for alloy deposited at 4 A dm^{-2}). So, on the basis of the chemical composition and results presented in Tables I and II it could be concluded that greater Fe amount in Zn–Fe alloy does not provide greater corrosion stability of these alloys. The differences in electrochemical properties among different Zn–Fe alloys rise from different chemical composition and surface morphology of alloys obtained at different current densities.[13] Namely, it is well known that Zn coatings deposited by different deposition parameters have differences in porosity, structure and other characteristics, which, in turn, affect the corrosion resistance of the coatings.[14]

As can be seen from Tables I and II, the Zn–Fe alloy deposited at 4 A dm^{-2} exhibited the lowest corrosion rate, *i.e.,* the longest time of red rust appearance (29 days) and the lowest j_{corr} (30 μA cm^{-2}), so this alloy was chosen for the modification of the steel surface prior to epoxy coating deposition. The electrochemical and transport properties, as well as the thermal stability of epoxy coatings electrodeposited on steel and steel modified by Zn–Fe alloy were investigated during exposure to 3 % aqueous NaCl.[15] On the basis of the results obtained by electrochemical impedance spectroscopy (EIS), gravimetric liquid sorption measurements and thermogravimetric analysis (TGA), it can be concluded that the properties of protective epoxy coatings are strongly influenced by the surface on which they are electrodeposited. Although the values of pore resistance are smaller for epoxy coating on steel modified by Zn–Fe alloy than for epoxy coating on steel, the Zn–Fe alloy layer could provide steel surface protection, postponing the time of electrolyte penetration to steel surface. This is pronounced during prolonged exposure time, when the pore resistance and charge-transfer resistance for epoxy coating on steel modified by Zn–Fe alloy remain constant over the long exposure time, due to the formation of a pseudo-passive layer of corrosion products mainly consisting of $ZnCl_2{\cdot}4Zn(OH)_2$,[16,17] which are a good barrier to the transport of water, oxygen and electrolyte ions. This behaviour is very similar to that of epoxy coating electrodeposited on steel modified by Zn–Ni alloys[18,19] and epoxy coating electrodeposited on steel modified by Zn–Co alloys.[20,21]

The higher value of diffusion coefficient of water (obtained by gravimetric liquid sorption measurements) and greater amount of absorbed water (obtained by TGA) for epoxy coating on steel as compared with epoxy coating on steel modified by Zn–Fe alloy, indicate the more porous structure and lower overall corrosion stability.[15] This could be explained by the existence of hydrogen evolved during electrodeposition of epoxy coating,

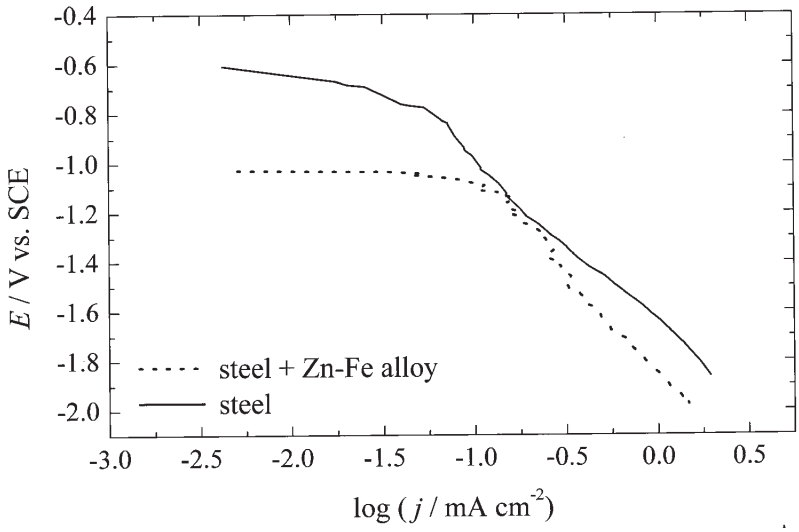

Fig. 5. Polarization curves for hydrogen evolution on steel and steel modified by Zn–Fe alloy, in polymer solution at 25 ºC, N_2 saturated (sweep rate 0.5 mV s^{-1}, 2000 rpm).

which due to the smaller wettability of steel surface (the contact angle on steel was 48º, while Zn–Fe alloy showed complete wettability),[15] and greater rate of H_2 evolution (Fig. 5) accumulates on the cathode. During the subsequent curing at 180 ºC of the epoxy coating, the H_2 goes out, leaving more vacancies in the polymer network and causing epoxy coating on steel to have a more porous structure. The larger amount of hydrogen accumulated on steel surface reacts with oxygen in the polymer chains causing an increased number of hydrogen bonds, and, consequently, the thermal stability for epoxy coating on steel is increased.[15]

CONCLUSION

The homogeneous and smooth Zn–Fe alloys were electrodeposited on steel at different current densities between 2 A cm^{-2} and 10 A dm^{-2} and temperature of 25 ºC. Chemical composition of Zn–Fe alloys was determined by EDX analysis using SEM and varied from 1.0 wt.%, for alloy electrodeposited at 2 A dm^{-2}, to 2.2 wt.%, for alloy electrodeposited at 10 A dm^{-2}. ALSV and XRD analysis were used in determining the phase structure of Zn–Fe alloys and it was shown that all alloys consist of one phase, Zn–rich η-phase independently of deposition current density. From j_{corr} values, estimated from polarization curves and time dependence of E_{ocp}, the corrosion properties of Zn–Fe alloys were investigated. The electrochemical measurements (E_{ocp}, j_{corr} determination) corresponded to that of visual observation (the time of red rust appearance). The influence of the plating current density in Zn–Fe alloys electrodeposition on the corrosion resistance of these alloys was shown. It was obtained that Zn–Fe alloy deposited at 4 A cm^{-2} exhibited the lowest corrosion rate, *i.e.,* the longest time of red rust appearance and the lowest j_{corr}.

Acknowledgements: This research was financed by Ministry of Science, Techologies and Development, Republic of Serbia, contract number 1689.

ИЗВОД

ЕЛЕКТРОХЕМИЈСКО ТАЛОЖЕЊЕ И КАРАКТЕРИЗАЦИЈА Zn–Fe ЛЕГУРА

ЈЕЛЕНА Б. БАЈАТ[1], ВЕСНА Б. МИШКОВИЋ-СТАЊКОВИЋ[1], МИОДРАГ Д. МАКСИМОВИЋ[1], ДРАГУТИН М. ДРАЖИЋ[2] и СЛАВИЦА ЗЕЦ[3]

[1]*Технолошко-металуршки факултет, Универзитет у Београду, п. пр. 3503, 11120 Београд,* [2]*ИХТМ-Институт за електрохемију, п. пр. 473, 11001 Београд и* [3]*Институт за нуклеарне науке "Винча", п. пр. 522, 11001 Београд*

Легуре Zn–Fe електрохемијски таложене на челику под различитим условима испитиване су применом анодне линеарне промене потенцијала и дифракције X-зрака, за одређивање фазне структуре, спектроскопије енергетски диспергованих X-зрака, за одређивање хемијског састава и поларизационих мерења као и мерења потенцијала отвореног кола, за одређивање корозионе стабилности. Проучаван је утицај густине струје таложења на хемијски састав, фазне структуре и корозиону стабилност Zn–Fe легура. Показано је да густина струје таложења веома утиче на корозиону стабилност Zn–Fe легура, и да легура таложена густином струје од 4 A dm^{-2} има најмању брзину корозије.

(Примљено 7. маја 2004)

REFERENCES

1. R. Fratesi, G. Lunazzi, G. Roventi, in *Organic and Inorganic Coatings for Corrosion Prevention Vol. 20*, L. Fedrizzi, P. L. Bonora, Eds., The Institute of Materials, London, 1997, p. 130
2. S. R. Rajagopalan, *Met. Finish.* **70** (1972) 52
3. M. Pushpavanam, S. R. Natarajan, K. Balakrishnan, L. R. Sharma, *J. Appl. Electrochem.* **21** (1991) 642
4. M. A. Pech-Canul, R. Ramanauskas, L. Maldonado, *Electrochim. Acta* **42** (1997) 255
5. W. Kautek, M. Sahre, W. Paatsch, *Electrochim. Acta* **39** (1994) 1151
6. Z. Zhang, W. H. Leng, H. B. Shao, J. Q. Zhang, J. M. Wang, C. N. Cao, *J. Electroanal. Chem.* **516** (2001) 127
7. V. Narasimhamurthy, B. S. Sheshadri, *J. Appl. Electrochem.* **26** (1996) 90
8. H. Park, J. A. Szpunar, *Corros. Sci.* **40** (1998) 525
9. S. K. Zečević, J. B. Zotović, S. Lj. Gojković, V. Radmilović, *J. Electroanal. Chem.* **448** (1998) 245
10. V. D. Jović, A. R. Despić, J. Stevanović, S. Spaić, *Electrochim. Acta* **34** (1989) 1093
11. *Metals Handbook, Vol. 8. Metallography, Structures and Phase Diagrams*, American Society for Metals, Ohio, 1973
12. *Powder Diffraction File, Inorganic Volume PD/S 5iRB, Sets 1-5*, American Society for Testing and Materials, Philadelphia, PA, 1969
13. K. Kondo, T. Murakami, K. Shinohara, *J. Electrochem. Soc.* **143** (1996) L75
14. S. Swathirajan, J, *Electrochem. Soc.* **133** (1986) 671
15. J. B. Bajat, V. B. Mišković-Stanković, Z. Kačarević-Popović, *Prog. Org. Coat.* **47** (2003) 49
16. M. R. Lambert, R. G. Hart, H. E. Townsend, *SAE Tech. Pap. Series No 831817*, Detroit, MI, 1983, p. 81
17. T. E. Graedel, *J. Electrochem. Soc.* **136** (1989) 193C
18. V. B. Mišković-Stanković, J. B. Zotović, Z. Kačarević-Popović, M. D. Maksimović, *Electrochim. Acta* **44** (1999) 4269
19. J. B. Bajat, Z. Kačarević-Popović, V. B. Mišković-Stanković, M. D. Maksimović, *Prog. Org. Coat.* **39** (2000) 127
20. J. B. Bajat, V. B. Mišković-Stanković, M. D. Maksimović, D. M. Dražić, S. Zec, *Electrochim. Acta* **47** (2002) 4101
21. J. B. Bajat, V. B. Mišković-Stanković, Z. Kačarević-Popović, *Prog. Org. Coat*. **45** (2002) 379.